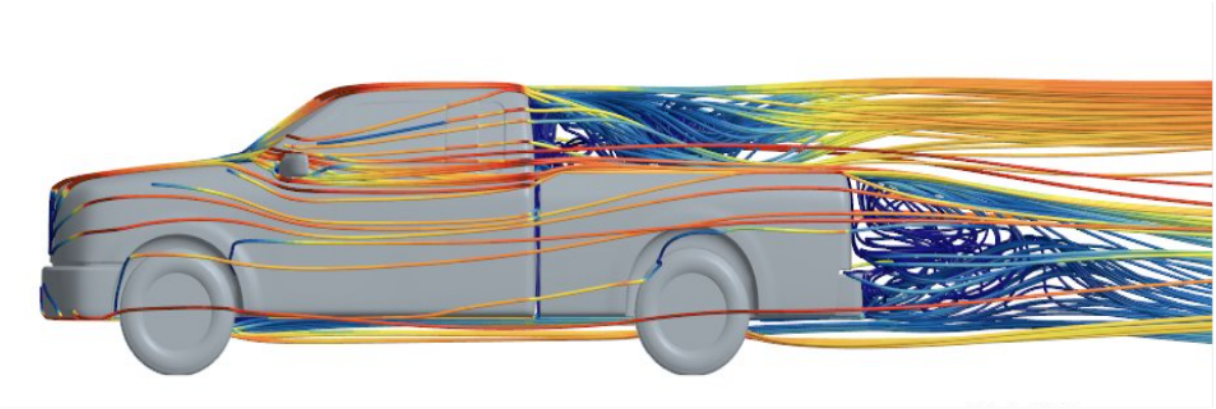

Aerodynamics investigations and optimization of a simplified pick-up truck with wind tunnel and CFD testing

Investigating the aerodynamics stability of the optimized pick-up truck in both straight air and side yaw wind

Master's thesis in Mobility Engineering

Karthik Yathiraj
Pavan Chaithanya

DEPARTMENT OF MECHANICS AND MARITIME SCIENCES
CHALMERS UNIVERSITY OF TECHNOLOGY
Gothenburg, Sweden 2024
www.chalmers.se

Master's thesis 2024

Aerodynamics investigations and optimization of a simplified pick-up truck with wind tunnel and CFD testing

KARTHIK YATHIRAJ, PAVAN CHAITHANYA

Department of Mechanics and Maritime Sciences
Chalmers University of Technology
Gothenburg, Sweden 2024

Aerodynamics investigations and optimization of a simplified pick-up truck with wind tunnel and CFD testing

KARTHIK YATHIRAJ
PAVAN CHAITHANYA

© KARTHIK YATHIRAJ
PAVAN CHAITHANYA , 2024.

Supervisor: Alexey Vdovin, Department of Mechanics and Maritime Sciences

Examiner: Alexey Vdovin, Department of Mechanics and Maritime Sciences

Master's Thesis 2024
Department of Mechanics and Maritime sciences
Chalmers University of Technology
SE-412 96 Gothenburg
Telephone +46 31 772 1000

Abstract

This master's thesis presents a comprehensive study on the aerodynamics and optimization of a simplified generic pick-up truck model through combined wind tunnel testing and computational fluid dynamics (CFD) simulations in StarCCM+. The primary objective is to understand and investigate the aerodynamic behavior of the generic pickup truck and design new attachments for the pickup truck on the trailer.

Based on existing knowledge, design optimization techniques were used to find design changes that could reduce aerodynamic drag. A flat underbody, a closed grill gap, and various rear attachments were among the changes made to the truck's shape. A comprehensive study and cross-validation of the suggested aerodynamic improvements were made possible by the combination of wind tunnel testing and CFD.

The ANSA software was used to optimize the CAD model. 3D printing was later used to create a 1/10 scaled-down model of the generic pickup truck, along with three distinct attachments called Flat back, Hatch back, and Fastback. Later tested the 3D printed model in Chalmers University of Technology's wind tunnel in Sweden. Drag forces were captured with the aid of wind tunnel experiments. These experimental findings served as a standard by which to validate the CFD models. The airflow surrounding the vehicle was then simulated using extensive CFD analyses using the StarCCM+ software.

The findings presented in this paper are the outcome of research and comprehension of the vehicle's aerodynamic behavior. They also show enhancements in the pickup truck's aerodynamic performance, with the quick back attachment lowering the drag coefficient. In addition to highlighting the potential for significant fuel and pollution reductions in pick-up trucks through aerodynamic optimization, this work shows how well experimental and computational methodologies may be used for aerodynamic investigations.

Keywords: Aerodynamics, Wind tunnel testing, Computational Fluid Dynamics, StarCCM+, Aerodynamic drag, Rear attachments, ANSA software, 3D printing, Flat bed, Hatch back, Fastback, Drag coefficient

Acknowledgement

We would like to express our gratitude to our supervisor and examiner Alexey Vdovin for his unwavering support and guidance throughout the course of this thesis. We also acknowledge the personnel at the XP and fuse labs for providing the necessary knowledge and documentation with respect to the operation of the 3D printers and the fuse lab for allowing us to use the paint booth.

Contents

List of Figures

List of Tables

Chapter 1

Introduction

1.1 Background

Enhancing vehicle performance, fuel efficiency, and overall sustainability is an ongoing goal for the automobile industry. Optimizing vehicle aerodynamics is essential to reaching these objectives since it has a direct impact on emissions, fuel economy, and stability. Due to their distinctive body forms and design elements, such the open cargo bed and upright front profile, pick-up trucks—which are renowned for their usefulness and versatility—present particular aerodynamic challenges.

Wind tunnel testing has long been a mainstay of aerodynamic development in automobiles, offering useful empirical data on drag forces, pressure distribution, and airflow behavior. However, conducting wind tunnel testing on its own can be expensive and time-consuming, especially when examining several design options. Aerodynamic studies have undergone a revolution since the development of Computational Fluid Dynamics (CFD), which complements experimental methods by providing precise simulation of airflow around complex geometries. CFD solves and analyzes fluid flow issues using numerical techniques and algorithms, providing insights into areas that are challenging to measure experimentally. When combined with wind tunnel testing, CFD offers engineers a potent tool for aerodynamic optimization that enables them to virtually test and develop vehicle designs repeatedly before building physical prototypes.

Even with CFD's breakthroughs, accurately predicting turbulent flows around vehicles is still difficult. As a result, combining CFD simulations with wind tunnel testing guarantees a greater degree of precision and dependability in aerodynamic research. This integrated method offers a strong framework for optimizing vehicle designs and enables comprehensive validation of computer models.

Increasing aerodynamics is especially advantageous for pick-up trucks. Aerodynamic drag reduction increases fuel efficiency, handling, and stability of the vehicle. The whole aerodynamic performance can be greatly impacted by design changes such improving the cab and bed's shape, adding aerodynamic aids, and fine-tuning under body combinations. This thesis uses both wind tunnel tests and CFD simulations to address the aerodynamic difficulties of pick-up trucks. The study's main objectives are to examine the aerodynamic behavior of a simplified pick-up truck model, find design modifications to lower drag and boost efficiency, and validate the computational results using experimental data. The

findings of this study could influence pick-up truck designs in the future, resulting in the creation of more ecologically friendly and fuel-efficient automobiles.

1.2 Purpose

This thesis project's main goals are to perform a thorough analysis of a simplified pick-up truck model's aerodynamics and to find efficient design modifications that can lower drag and increase fuel economy. Thorough the integration of wind tunnel experiments with Computational Fluid Dynamics (CFD) models, the specific goals of this research are as follows:

Create a Framework for Methods: This will provide a solid methodological foundation for doing our thesis with a combined CFD and wind tunnel investigations related to automobile aerodynamics and also illustrate the advantages of combining computational and experimental methods for optimizing vehicle design.

Enhance Aerodynamic Architecture: This advantages us to investigate several design tweaks—like under body structure modifications, trying new configurations like flat back, hatchback, and fastback, that are intended to reduce aerodynamic drag and finally to assess the efficacy of these design modifications using wind tunnel testing and iterative CFD simulations.

Examine the Aerodynamic Properties: This provides us to use wind tunnel, to examine the drag forces, pressure distribution, and airflow patterns operating on a scaled-down pick-up truck model. to comprehend the truck's geometrical characteristics affect and its overall aerodynamic performance.

Verify Computational Frameworks: To create comprehensive computational fluid dynamics (CFD) models of the pickup vehicle and verify these models using empirical data gathered from wind tunnel testing. to evaluate the various turbulence models that were employed in the CFD simulations for correctness and dependability.

1.3 Thesis Project Outline

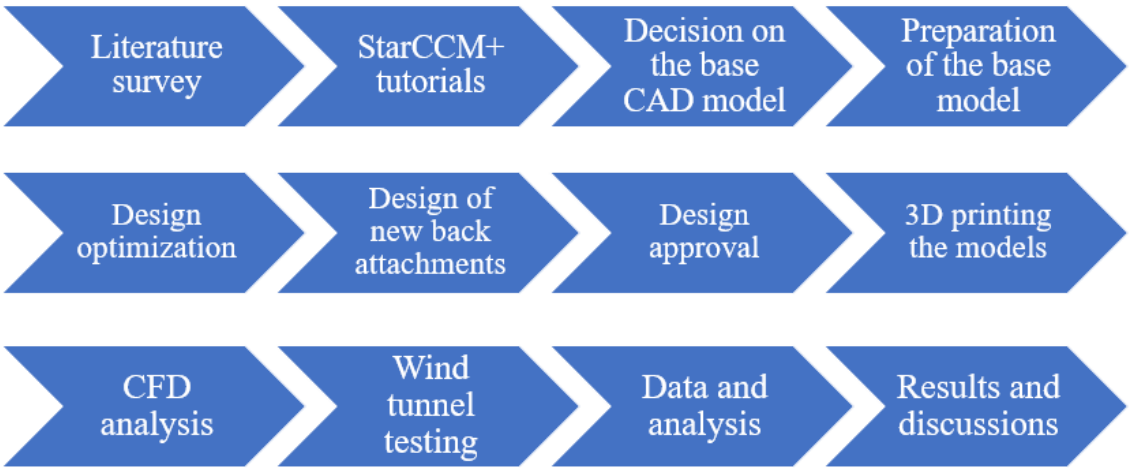

Figure 1.1: Project Framework

Chapter 2

Aerodynamics Theory

2.1 Drag

Aerodynamic drag is the component of drag that acts in the direction that is opposite to the direction of motion of a vehicle, predominantly caused by the difference in pressure in front and behind the body. The drag produced depends on the frontal area A_f, the Coefficient of drag C_D and the speed of the airflow V squared.

$$F_D = \frac{\rho A_f V^2 C_D}{2} \tag{2.1}$$

2.2 Coefficient of Pressure

The pressure coefficient is a non dimensional measure of pressure. It is obtained by the net difference between the pressure at the point of interest and the free stream pressure, normalized by the free stream dynamic pressure.

$$C_p = \frac{p - p_\infty}{\frac{\rho V_\infty^2}{2}} \tag{2.2}$$

2.3 Wall Y+

The Wall Y+ is a dimensionless parameter that can be used to calculate the distance of the first cell from the wall in a CFD simulation. y represents the distance from the wall to the location of interest within the flow, u_τ is the friction velocity, ν is the kinematic viscosity of the fluid.

$$y^+ = \frac{y u_\tau}{\nu} \tag{2.3}$$

2.4 General Transport equations

Equation 2.4 describes how the value of an arbitrary scalar quantity ϕ in a fluid domain is influenced by various parameters. The first term describes how ϕ changes with respect to time, the second term describes how ϕ changes due to convection in a fluid domain. The right hand side terms describe how ϕ changes in space influenced by the fluid parameter α and finally due to a source S_ϕ. These equations form the base for the naiver stokes equations that are solved during every CFD simulations.

$$\frac{\partial(\rho\phi)}{\partial t} + div(\rho\phi u) = div(\alpha grad(\phi)) + S_\phi \tag{2.4}$$

Chapter 3

Literature Survey

It is crucial to comprehend vehicle aerodynamics, especially pick-up truck aerodynamics, in order to improve overall performance, lower emissions, and increase fuel efficiency. Pick-up truck design elements, such the open cargo bed and vertical front profile, present particular aerodynamic issues. In order to identify important discoveries and gaps in the present understanding, this literature review examines previous studies and approaches pertaining to vehicle aerodynamics, with an emphasis on wind tunnel testing and Computational Fluid Dynamics (CFD) simulations.

The majority of vehicle aerodynamics research has been done on passenger automobiles; pick-up trucks have received less attention. The airflow separation at the back end of pick-up trucks, the airflow in the open cargo bed, and the design of the cab and front grille all have a big impact on their aerodynamic performance. Foundational insights into the general principles of vehicle aerodynamics, particularly the significance of lowering drag to improve fuel efficiency. Cab and Bed contact: Complex flow patterns are produced by the cab's contact with the open cargo bed, which increases drag. Aerodynamic drag can be greatly reduced by changing the design of the bed and adding covers and other back attachments such as hatchback and fast back.

Testing in Wind Tunnels: Aerodynamic research still relies heavily on wind tunnel testing to provide empirical data on pressure distribution and airflow behavior around vehicle models. Scale Model Testing: significance of simulating real-world situations in a controlled setting with scale models. Research conducted has confirmed that scale model testing is a reliable method for forecasting the behavior of full-size vehicles.

Computational fluid dynamics, or CFD, is a potent technique that may be used to simulate aerodynamic behavior and provides in-depth information to supplement wind tunnel testing. Notable advancements in the discipline comprise.

Simulation Accuracy: The numerical techniques and turbulence models employed determine how accurate CFD simulations are. Verification and Validation: It is essential to validate CFD models using experimental data. To guarantee the accuracy of CFD predictions, comprehensive validation and verification procedures are crucial Application to Pick-Up Trucks: Several design improvements to reduce drag have been investigated in CFD studies specifically for pick-up trucks. These studies demonstrate how CFD may be used to test several design iterations.

Chapter 4

Methodology

The following section talks about the design, manufacturing and simulation methods undertaken over the duration of this project.

4.1 Base Model

The European Car Aerodynamic Research Association (ECARA) produced the Base Model, also referred to as the Generic Truck Utility model. Car design trends have changed a lot since the model was first created, so an updated, excellent, open-access model is required to properly depict these developments. The Generic Truck Utility model has features found in most contemporary pickup trucks, especially in terms of bed and cab proportions. There are eighteen distinct combinations available for this type, including long cab with short box, medium cab with medium box, and short cab with long box. We decided to evaluate the aerodynamics of the medium cab with the medium box layout. This selection offers a fair representation and a standard by which to compare aerodynamic gains in various sizes. It provides a standard reference point, making it easier to gauge the effectiveness of design changes in different configurations.

The under body region of Generic Truck Utility model consists of the engine compartment, suspensions, axles, driving shaft, and chassis. The under body of the pick up truck has been simplified to flat under body as the study is more concentrated on the aerodynamic behaviour of vehicle due to change in box design and also for ease of manufacturing and simulation.

4.2 Box Design

The changes in the design of the box or new box attachments follow clear guidelines. Some parameters serve as control variables and must be consistent across the box attachment design to make them comparable in the wind tunnel study and simulations. In the case of the Generic Truck Utility, the base line design is kept constant for the box attachments. The body designs are based off of a flush body where uneven surfaces, such as the grills, are flushed with the rest of the body. This body design has done to avoid air flow into

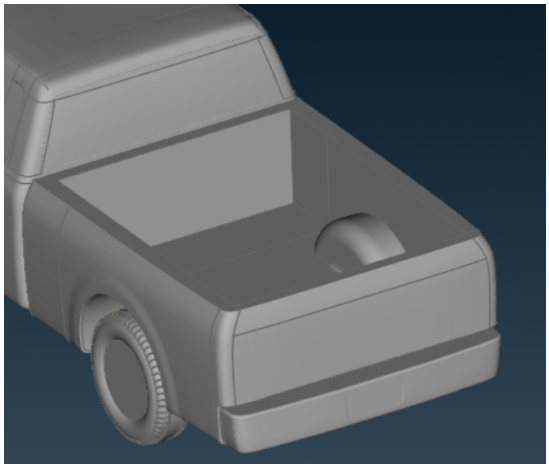

(a) Base model box.

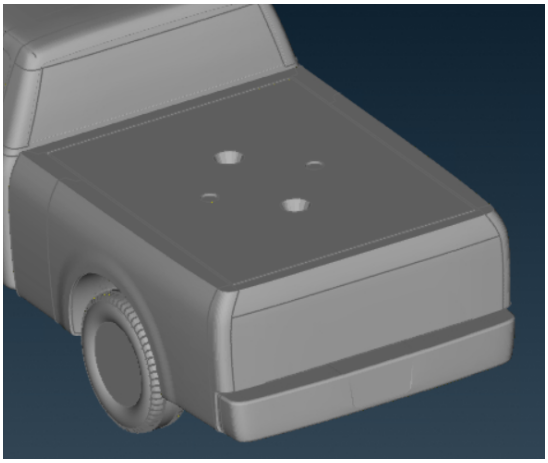

(b) Flatback Box.

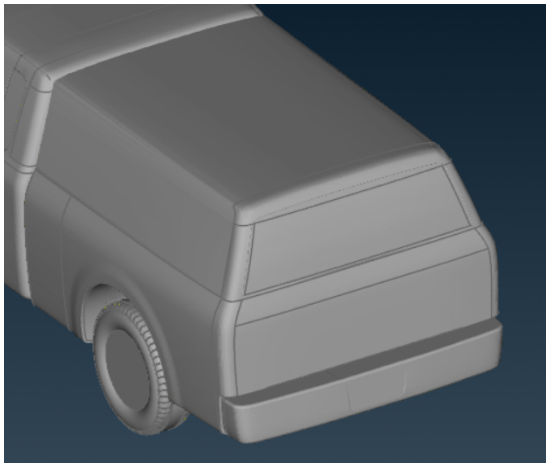

(c) Boxcap box.

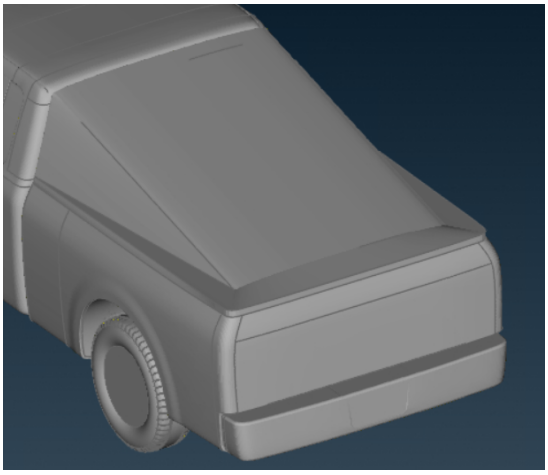

(d) Fastback.

Figure 4.1: Box attachment designs.

the under hood.

The surface of the caps is a crucial component in guiding the airflow smoothly around the body. The new caps were specifically designed to provide a smooth transition for the airflow. In the initial stages of design we decided to do modifications in Catia but we faced the limitation in file format which was nor suitable neither converted to editable format.

The box attachments are of three configurations. The first configuration is the flat box which covers the open box area which can be seen in the above figure 4.1b, second configuration is box cap the cap in the shape of hatch back covers the open box area as shown in the figure 4.1c and final configuration is the fast back where the fast back shaped box cap will cover the open box area which can be seen in figure 4.1d.

During the study in the belief of reducing the drag count of the pickup truck we designed the three different box caps. As the new designs improves the wake balance of the pickup truck. A challenge inherent to this configuration is the mounting of the box caps on the box where the box walls were very thin to have any mounting configurations for the caps.

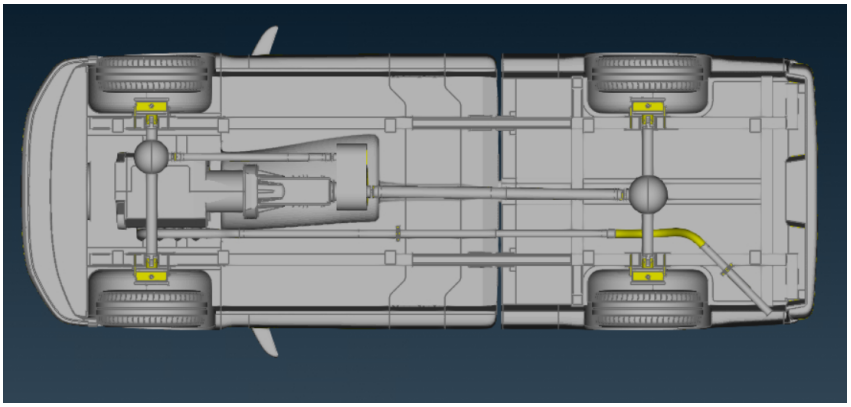

Figure 4.2: Under Body designs

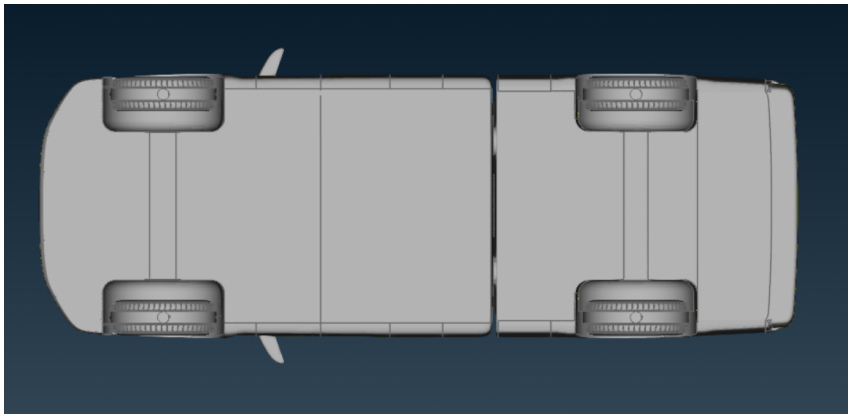

Figure 4.3: Flat Under Body designs.

4.3 Under body Design

The Generic Truck Utility model is given as a series of ANSA files. These ANSA files are imported into ANSA where they can be modified accordingly, using surface mesh functions. The under body of the pickup truck was modified to have a flat body as in the figure 4.2 to where the model we started with had the engine, drive shaft, suspension components, differentials, exhaust and chassis which can be seen in figure 4.3. All the under body components were deleted and wheel arches were modified to fill the gaps of the suspension and similar trend is followed in the under body and a we can see the step in the under body to this was created to accommodate the mounting of the wheel to the body.

4.4 Design for manufacturing

4.5 Body

To ease the printing process the main body of the pickup truck was divided into three specific parts: front cab, rear cab and box.The engine compartment and interior components were stripped from the cab.

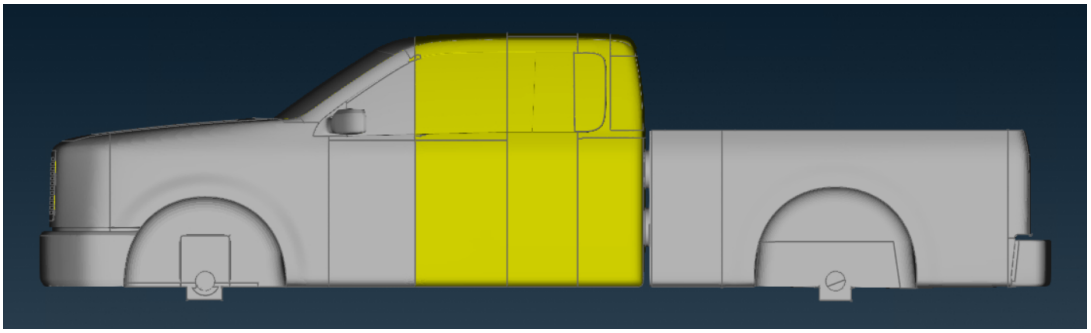

Figure 4.4: Body split

Slots and protrusions between the surfaces were used to help maintain alignment of the 3D printed parts as well a structural rigidity. These advancements help to make the parts fit together perfectly. Components, when aligned are bonded to one another by means of an adhesive and become secured in position forever.

4.6 Wheels

The rims of the wheels has been closed to avoid the air flow through the wheels. This simplification is done as we do not have spinning wheels in the experimental setup and want therefore to minimize its influence on the aerodynamic drag. The holes to mount the truck inside the wind tunnel is also placed on the circumference of the wheels at it is the part of the truck which is close to the ground. The wheels are modified to the above design seen in figure.

4.7 3D-Printing

The scaled physical model of the Generic Truck Utility mode was entirely 3D printed using PLA (Polylactic acid) due to its superior surface finish and resistance to thermal related issues such as warping, which is favorable for large prints such as this. Thermal warping is caused due to the non uniform cooling of the lower layers that results in the bottom layers contracting and lifting off the base plate. PLA also allows for a more precise and detailed print, as the plastic is not susceptible to fluctuation in the printing environment. The downside to using PLA is its fragility, which has been taken into account by printing more vertical walls.

Initially there was an opportunity to use 2 different printers, the Prusa MK3s and the Creality Cs10v5. We observed that although the printing time was vastly reduced in the creality printer, this came at the expense of poor surface quality and the parts were especially prone to temperature related warping issues as the lifting edges. For this reason the Prusa MK3s was chosen for all subsequent prints of the body. The prusa yields a superior surface finish due to the 0.6mm nozzle diameter compared to the 0.6mm nozzle in the Creality. Due to the limitations in the volume of printing section on the prusa, the main body had to be split into 3 parts to accommodate the prints as seen in figure 4.4. The prusa MK3s proved to be a robust and reliable 3D printer for the sections of the body with some sections taking over 32 hours to print.

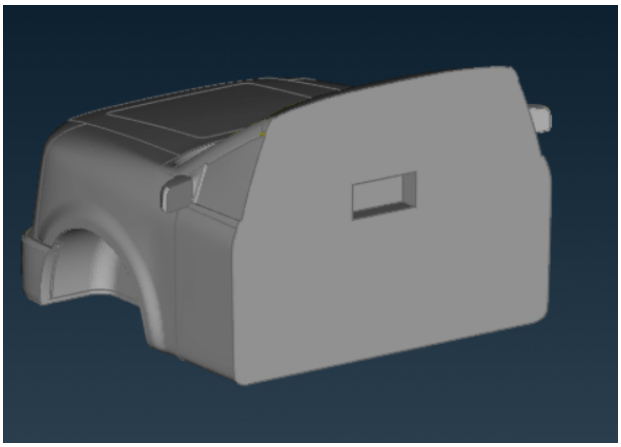

(a) Box Female.

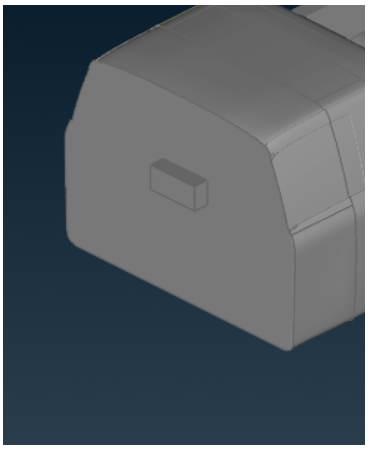

(b) Cab Male.

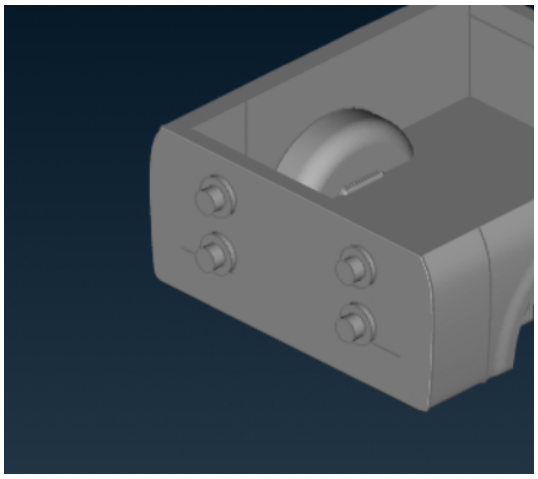

(c) Box Male.

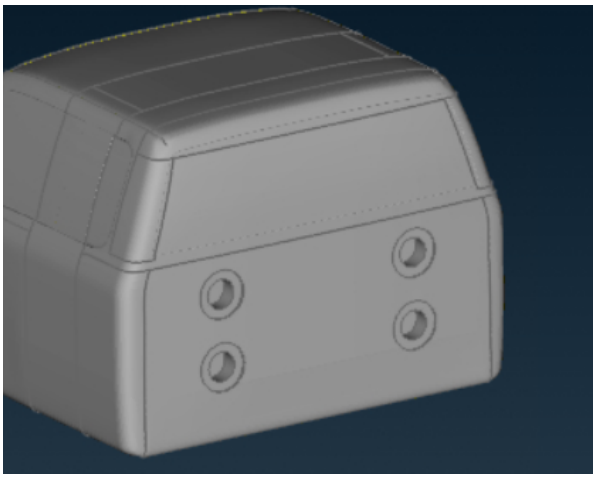

(d) Box Female.

Figure 4.5: Body attachment designs.

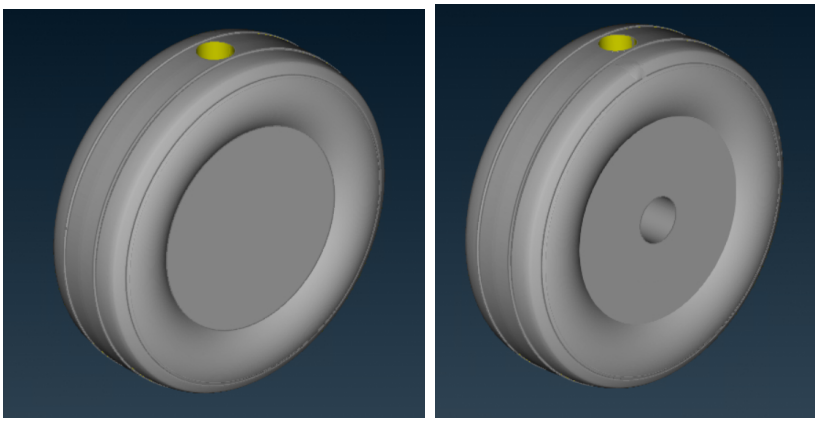

Figure 4.6: Simplified wheel designs.

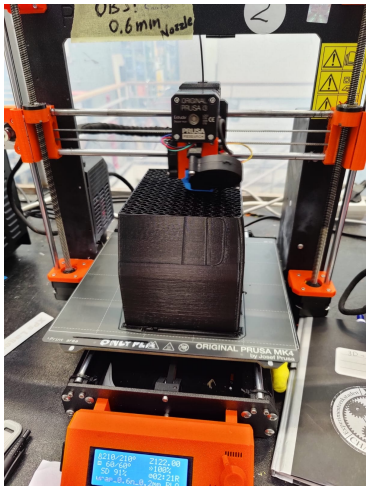

(a) 3D Printing front section of the body

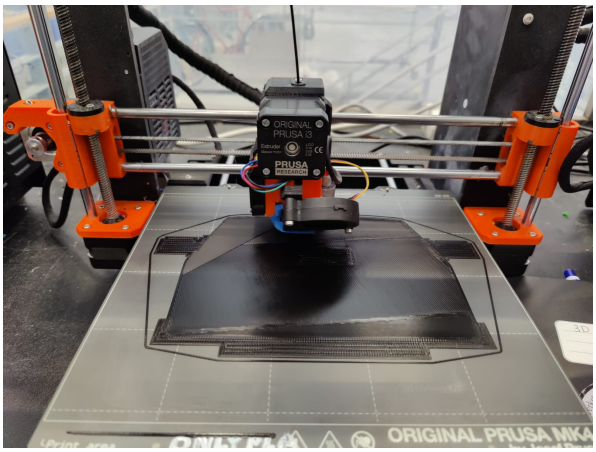

(b) 3D printing the mid section of the body

Figure 4.7: 3D Printing using the prusa MK3S

PETG is used as a substitute if the PLA is not available. The parts that are printed using PETG, the finish and detail is noticeably worse. Due to the detail and precision needed for models in the wind tunnel, PETG is not the most optimal printing material. This decision will lead to less post-processing of each part, allowing the group to focus on more important aspects. To obtain even finer parts, more expensive material could be purchased, however, the level of detail needed can be achieved using post-processing techniques, therefore it is not necessary.

Table 4.1: General 3D printing settings

Parameter	Value
Infill	10-15%
Infill type	Gyroid
Nozzle diameter	0.6mm
Layer height	0.1mm - 0.3mm
Number of walls	2-4
Support Type	Everywhere

4.8 Assembly

Since the body had to be printed in 3 separate sections, they had to be glued together manually. This inevitably led to a poor and inconsistent surface finish on the perimeters of the glued faces. This had to be rectified using spackel paste which adds additional material that can be easily sanded down. The wheels were glued to a M10 screw and was threaded into the hole in the wheel hub, extending into the body. This was done to strengthen the axle to withstand the down force created when the car tested in wind tunnel and to allow the adjustment of the mounting holes by rotating the wheels about its axis.

4.9 Surface preparation

I order have a smooth texture finish on the 3D printed components, the parts were undergone for surface preparation. Firstly all the models were stuck to each other based on the modality using super glue and let that rest for a day. Followed by sanding the model starting rough sanding to smooth sanding. During the sanding the process we were able to remove ridges and minute deposition on the printed parts and achieved the smooth finish.

After sanding process the the parts were painted with two coats of primer and let it dry for some while, followed by two to three coats acrylic black spray paint was applied on all the parts. Finally, finishing of the surface preparation by applied two to three layers of clear coat. Clear coat helped us to get better surface finish and improved surface appearance. The different steps of post processing can be seen in the pictures a to c in figure 4.8.

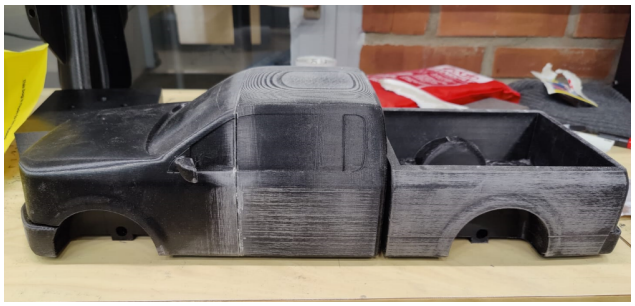

(a) Gluing the body and sanding

(b) Vehicle body being primed for painting

(c) Vehicle after surface preparation

Figure 4.8: Surface Preparation

Chapter 5

Simulation Model

5.1 CFD Simulations

The simulation model, which comprises the full-scale pickup truck model and the computational domain, is configured using StarCCM+. This section's primary focus is on the process of creating the simulation file for the CFD investigation. Because it requires a careful selection of numerous settings that directly affect the accuracy and reliability of our simulations, this phase was crucial to the success of our project.

5.2 Simulation setup

Software called Simcenter StarCCM+ 2022.1 was used to do the CFD analysis. A full-scale import of the pickup truck is made. Here is a synopsis of the setup process. The physics of the simulation is defined as follows:

5.2.1 Steady flow

This study used the steady state technique. Compared to transient flow simulations, it is better suitable for our design studies due to its comparatively shorter runtime.

5.2.2 Constant density

In constant density the Mach-number can always be considered low (< 0.3). The flow can therefore be considered incompressible, its density constant, and equal to that of air.($1.18415\ kg/m^3$).

5.2.3 K-Epsilon Turbulence model

The most resilient and dependable model for turbulent flows is the K-Epsilon model. This offers a good trade-off between accuracy and computing efficiency. The Realizable Two-Layer K-Epsilon model, which combines the Realizable K-Epsilon model with the two-layer technique, has been employed more precisely.

5.2.4 Two-Layer All y+ Wall Treatment

This treatment is used to capture the near-wall flow physics accurately.

5.2.5 Initial Conditions

The following initial conditions are set:

- Pressure: 101325 Pa
- Static Temperature: 300 K
- Velocity: 30 m/s

5.3 Coordinate System

The Pick-up truck model is placed within exactly in the Cog of the truck with the coordinate system. The length of the car in X-direction from the front end to the rear end. The Y-direction lies along the width of the truck towards its right side. The positive Z-direction aligns with the height of the vehicle, pointing upwards. Additional coordinate systems has been defined for the front wheels and rear wheels, so that the angular velocity can be defined for the wheels that matches the inlet velocity of the domain and the road.

5.4 Computational Domain and Boundary Conditions

The dimensions of the pick-up truck is as shown in the table5.1, and the dimensions of the computational domain are shown in table 5.2

Table 5.1: Pick-up Truck Size

Length (L)	Width (W)	Height (H)
5.24 m	1.82 m	1.65m

Table 5.2: Domain Size

Length	Width	Height
94.32 m	18.2 m	13.1 m

Boundary conditions applied to the computational domain.

- **Inlet:** The inlet velocity being at 30.0 m/s
- **Outlet:** Pressure outlet is defined
- **Road:** Moving ground
- **Walls:** Sides and roof

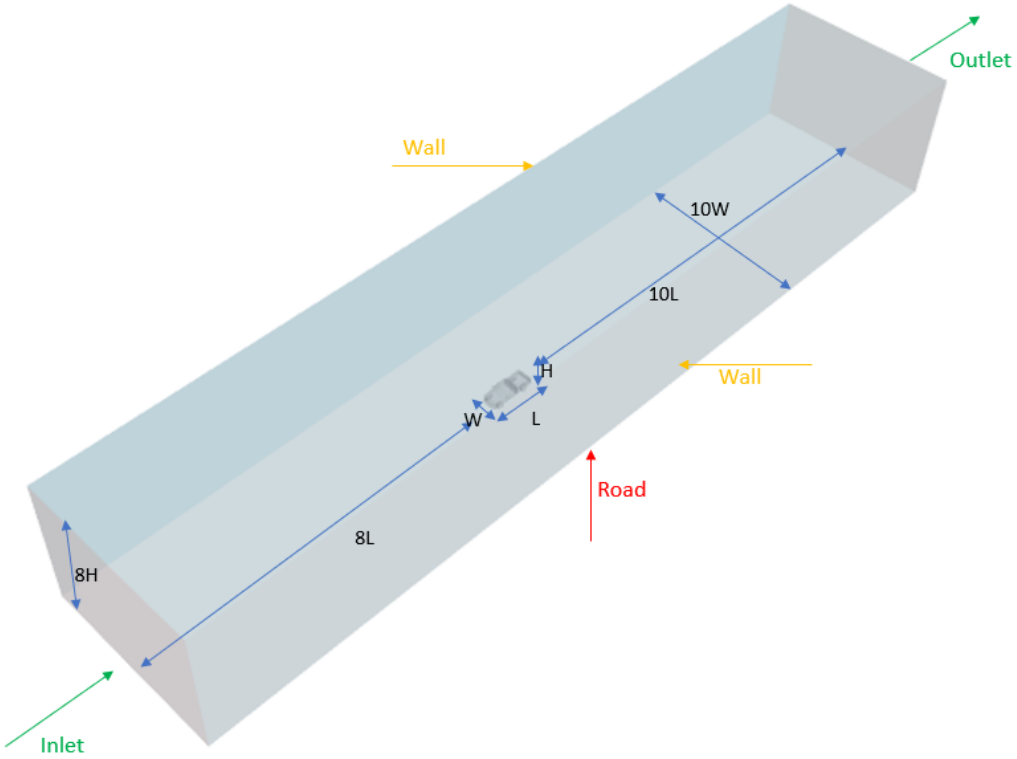

Figure 5.1: Computational Domain

- **No slip walls:** Outer surfaces of the pickup truck body

5.5 Computational Mesh

5.5.1 Surface wrapper

Using of the surface wrapper geometry tool during the simulations helps in cleaning complex geometries. When working with CAD models or surface models that contain gaps, overlaps, or other topological problems, this tool is quite helpful. By ”wrapping” a fresh, clean surface over the current geometry, the surface wrapper fixes these problems and prepares the model for mesh production. In our model we have used several surface custom control to define the exact geometry of the imported model. The general stetting for the surface wrapper is stated below.

Table 5.3: Surface Wrapper settings

Base size	Target surface size	Gap closure size
32.5 mm	0.0163 m	0.001 mm

Within the computational domain, a well defined flow domain is created using the ’Subtract’ operation tool. This means that the truck’s volume is subtracted from the computational domain’s volume, which defines the area where the flow passes through the

surfaces of the truck. It is now possible to construct the mesh. The volume domain mesh and the surfaces mesh employ different models.

5.5.2 Automated Mesh Operation

Surface Re-mesher

In order to enhance the quality and optimize volume mesh, this model triangulates the initial surface. The surface re-mesher's inputs values change according to the part surface. In order to capture as much of the flow behavior as possible, the goal is to reduce the mesh cell size in areas of interest while maintaining a larger cell size for the domain boundaries where the flow characteristics are simpler. This is accomplished by establishing refining zones, where the surface growth rate value controls the transition of various cell sizes in various truck parts, smaller cells are located on the side mirror surfaces and the wheel surfaces.

Automatic Surface Repair

This feature automatically fixes of geometric issues that could be present in the re-meshed surfaces, either by deleting the broken surface or by re-meshing it.

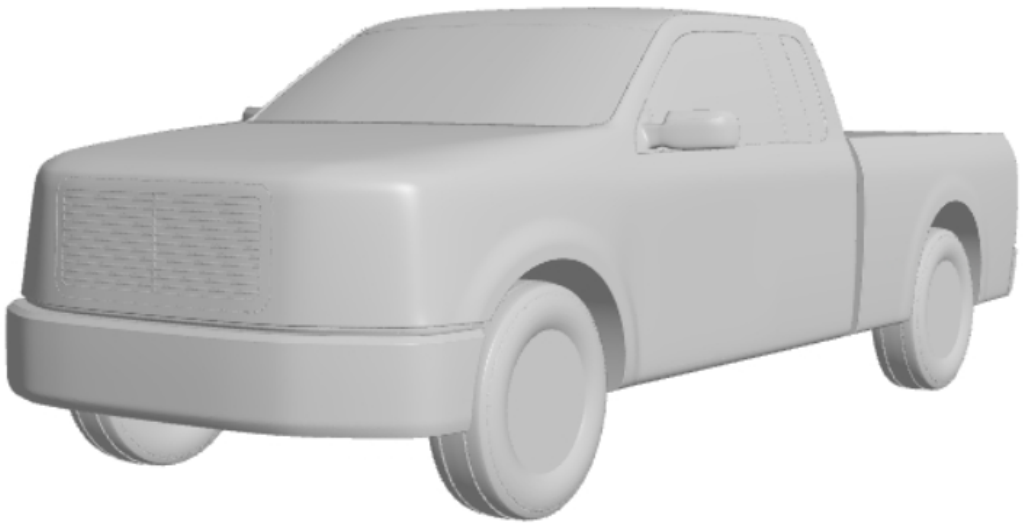

Figure 5.2: Surface Mesh

5.5.3 Volume Mesh

The following types of meshing models are used to create the volume mesh.

Trimmed Cell Mesher

Although the other models that are available have been shown to use less memory, the trimmed cell mesher has been chosen for its superior accuracy and outcomes. This mesh-

ing type creates a sturdy, high-quality grid with little cell skewness. Depending on the goal, we can create volumes of our specific interest and customize them under more stringent guidelines (such as altering the base size and volume growth rate). We have constructed four refinement zones in addition to the volume areas that are fixed to the truck's surface. Two offset volumes are made all around the vehicle to capture the characteristics of the flow, and two larger block volumes are required primarily to capture the wake behavior and yaw wake behavior of the rear.

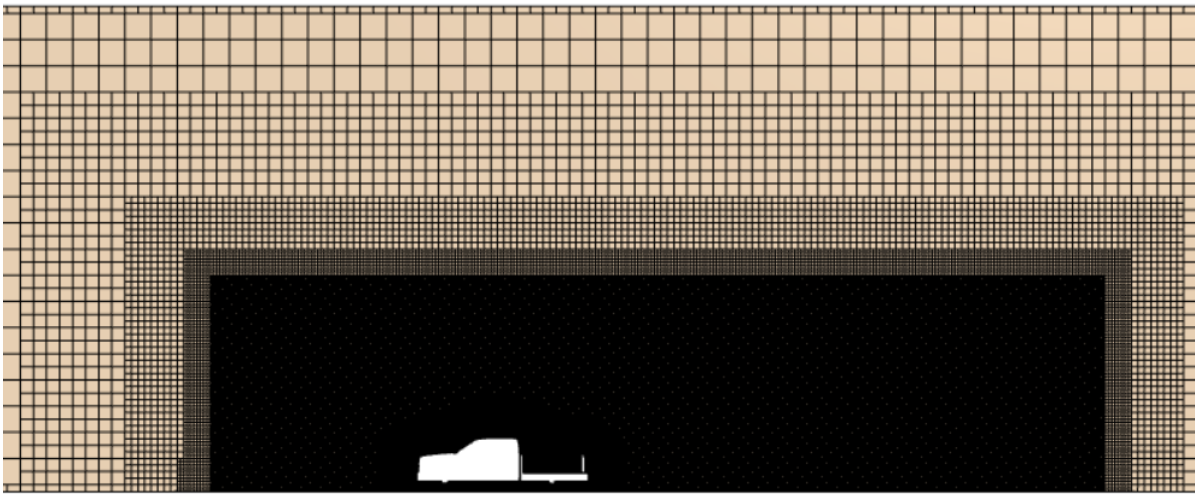

(a) Volume Mesh - Refinement zones

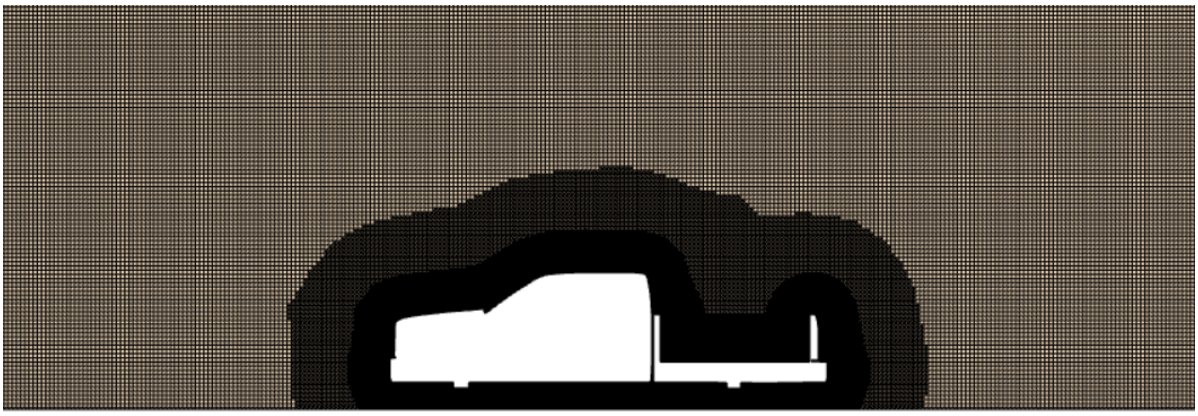

(b) Volume Mesh - Refinement zones

Figure 5.3: Volume Mesh

Wall Y+

The Y+ values range from 30 to 300, and the model employs a high Y+ approach. The main justification for selecting the high Y+ approach is the high computational cost of solving for a Y+ of less than 5, particularly in a scenario such as this one where pressure dominance is greater than shear dominance. An extremely precise set of mesh parameters for the prism layers was used to create the final mesh. The prism layer's overall height was fixed up-to 10 number of layers. The size of the global base has no

bearing on this. To properly resolve the near wall flow, a prism layer mesher is required. By constructing orthogonal prismatic cells adjacent to the wall surfaces, this is achieved. The final simulation results will depend on the thickness, size, distribution, and number of cell layers. These parameters must be chosen in order to anticipate the flow separation features with accuracy. The y+ argument must be added in order to accomplish this. When compared to the thickness of the viscous sub-layer in the boundary layer, it gives information on the relative size of the initial grid cell close to a solid surface. A high y+ method ($30<y^{+}<300$) is advised for this investigation since it offers a fair trade-off between computational expense and accuracy of the simulation.

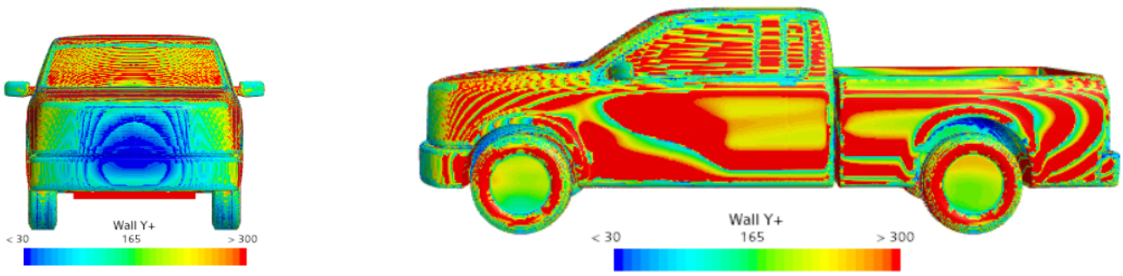

(a) Wall Y+ Front View

(b) Wall Y+ Side View

Figure 5.4: Wall y+

Custom mesh controls

Custom controls must be applied to the geometry and domain for the size and number of prism layers, as not all sections within the domain require the same base size mesh configuration.

Table 5.4: Custom Mesh Controls

Region	External Body	Ground	0.5m Offset	1.2m Offset	Ref. Block 1	Ref. Block 2
Base size (Absolute)	100mm	N/A	15mm	30mm	60mm	80mm
Number of Prism Layers	5	0	4	4	4	4

Stopping Criteria

The simulation stops when one of the following criteria is met.

- **Drag coefficient monitor criteria:** The simulations were used to terminates when the value of the drag coefficient remains within a 0.001 difference range from the previous 400-600 iterations.

- **Maximum number of iterations:**: All of the base configurations' simulations were done through 1600–2000 iterations. The halting criteria with asymptotic limit was introduced to the simulations during the yaw angle condition, which caps the asymptotic behavior of the iterations in the drag coefficient models up to a predetermined number of 600 samples.

Chapter 6

Wind Tunnel Test

6.1 Wind Tunnel Theory

Chalmers scaled wind tunnel served as the venue for the wind tunnel testing. This wind tunnel is a closed return type that runs at a maximum speed of $63m/s$ thanks to a fan with six blades that is powered by a 170kW electric motor. The test part is $3m$ in length and $2.25m^2$ in size.

The flow pattern and velocity distribution of the flow around and downstream of a test object are changed when it is positioned in the test section. To get the true force coefficients, obstruction effects caused by walls must be corrected for. One way to express the correction factor is as

$$C_{d,True} = C_{d,Indicated}\Big(1 - \frac{A}{S}\Big)^{1.228} \tag{6.1}$$

An external balance with four mounting points one for each corner of the model that is part of a six-component strain gauge type is used to measure the forces and moments. In order to determine the pitching moment and the lift forces, the struts can therefore be changed to suit the wheelbase and track width of a test object. Crosswinds and yaw may be replicated by rotating the external balance on its own axis.

6.2 Pickup Truck Wind Tunnel Testing

To record the performance of the scaled model (1:10) of the 3D-printed Pick-up truck model was put to the test in the Chalmers Wind Tunnel, we had four configurations to be tested in the wind tunnel one base model with three different attachment as shown in the figures below. We used aluminum tape to seal any gaps in the printed model, such that it prevents any undesired air leakage and ensuring accuracy. The model was safely fastened to the wind tunnel with the help of balancing plate. so that we get accurate measurements of drag, density and velocity of the air inside the wind tunnel.

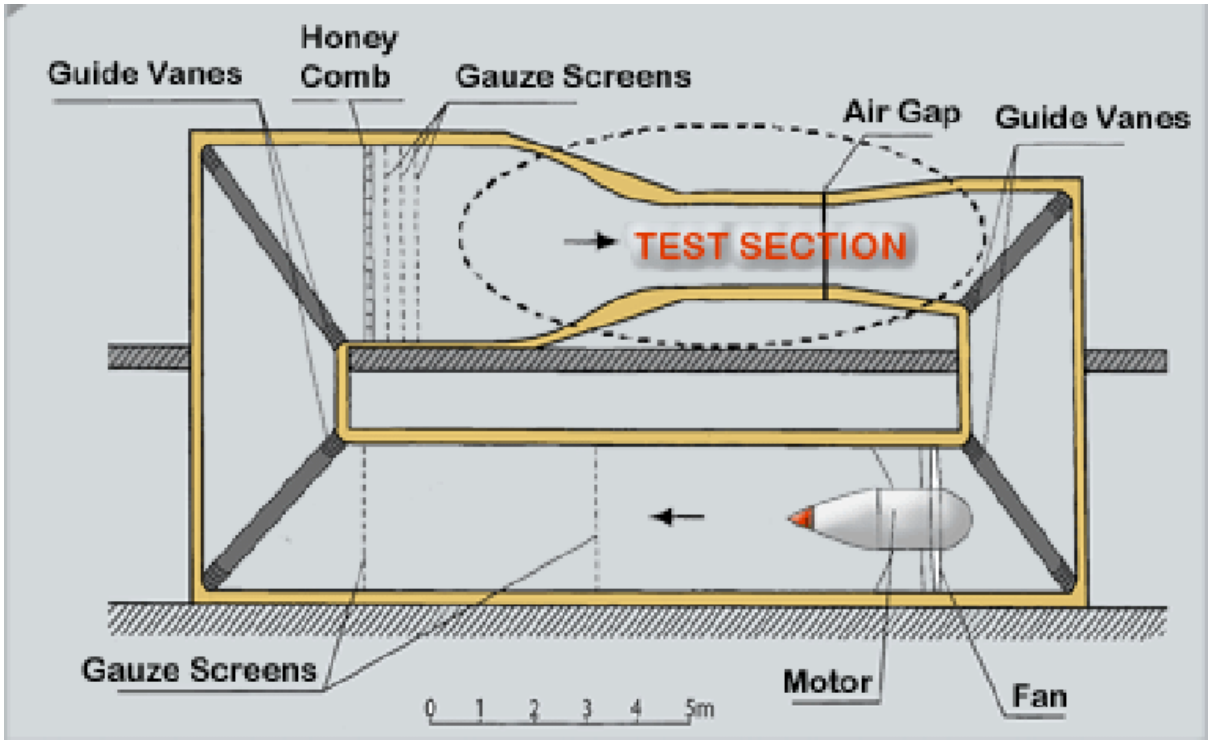

Figure 6.1: A Schematic of the Chalmers Wind tunnel

(a) Base model configuration

(b) Flat bed configuration

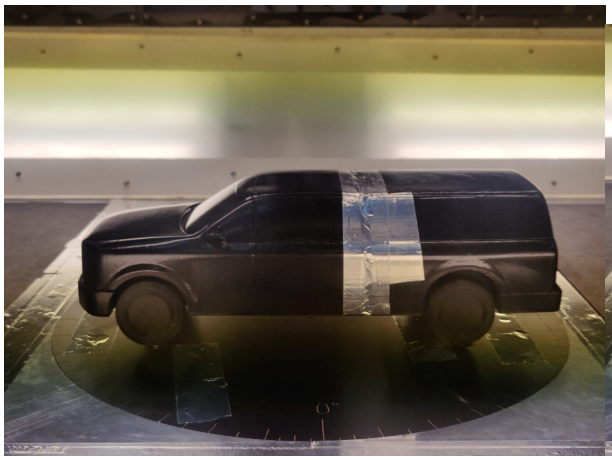

(c) Hatch Back configuration

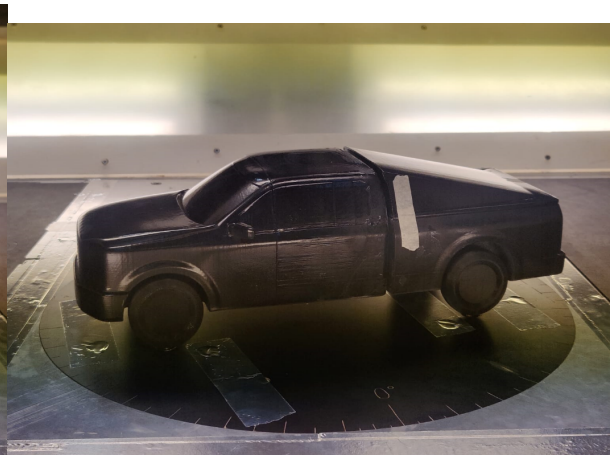

(d) Fast Back configuration

Figure 6.2: All configurations wind tunnel testing.

6.3 Reynolds Sweep

A Reynolds sweep in aerodynamics can be used to evaluate how various airspeeds, which vary the Reynolds number, impact a wing's or vehicle's performance. For designs to be optimized for both high-speed and moderate speed circumstances, this is crucial.

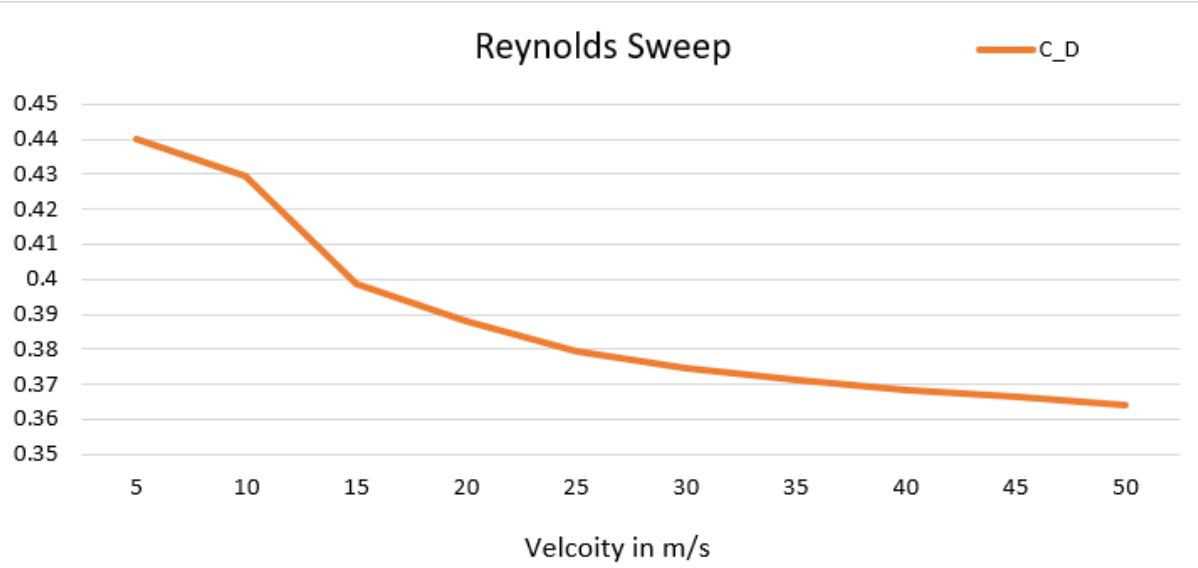

Figure 6.3: Reynolds Sweep for the base model

Figure 6.3 illustrates how the C_d decreases with increasing wind speed. We have chosen to 30 m/s as the testing speed for our wind tunnel testing for all the models to conserve energy.

6.4 Configurations Tested

We have in total of four configurations which is first one being the base model as shown in 6.2a and with three different back attachments see Figure 15, the second configuration is the flat bed model, where the trunk part is cover with flat surface 4.1d, the third configuration is the Hatch back model6.2c and the last one is the fast back model configuration 6.2d

6.5 Post-Processing and Wind Tunnel Data

1. Coefficients
    - *Drag Coefficient*: C_d
    - *Drag Force*: F_x in N
    - *Frontal Area*: A in m^2

- *Velocity*: V in m/s
- *Air Density*: ρ in kg/m^3

2. Coefficient Calculations

$$C_d = \frac{F_x}{0.5\rho A V^2}$$

Chapter 7

Results

7.1 CFD Simulation

7.2 Pressure Coefficient

The concentration of a fluid on a vehicle's body can be roughly estimated using pressure coefficient graphs; the higher the pressure coefficient, the more stagnation there is in the fluid. A positive Cp value indicates that the fluid is pushing against the solid's surface. On the other hand, a pulling force on the solid surface is indicated by a negative value of Cp. As a result, the entire stagnation area is located on the pickup truck's front grill.

Figure 7.1: Base model Configuration Views

(a) Front View

(b) Rear View

Figure 7.2: Flat Bed Configuration Views

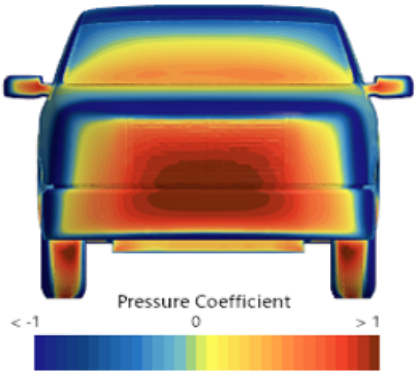

(a) Flat Bed - Front View

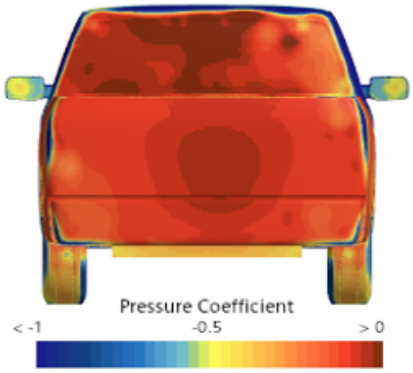

(b) Flat Bed - Rear View

Figure 7.3: Hatch Back Configuration Views

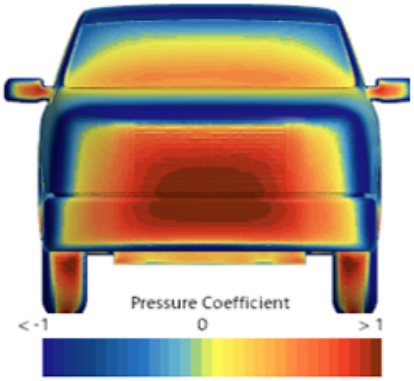

(a) Hatch Back - Front View

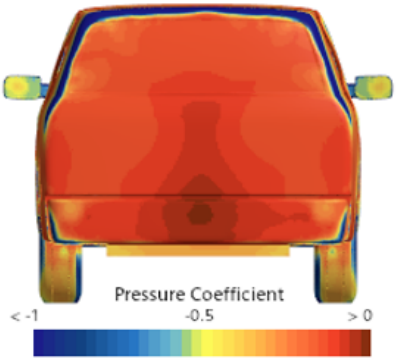

(b) Hatch Back - Rear View

Figure 7.4: Fast Back Configuration Views

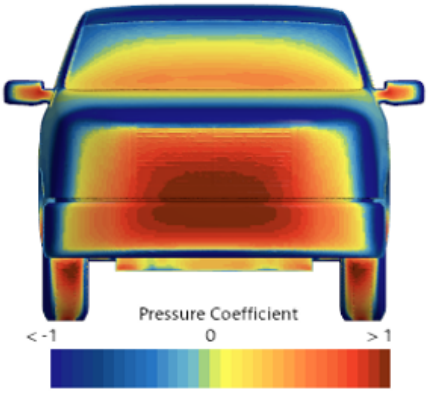

(a) Fast Back - Front View

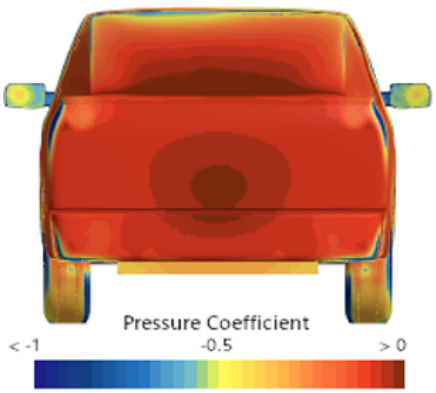

(b) Fast Back - Rear View

7.3 Velocity Vector

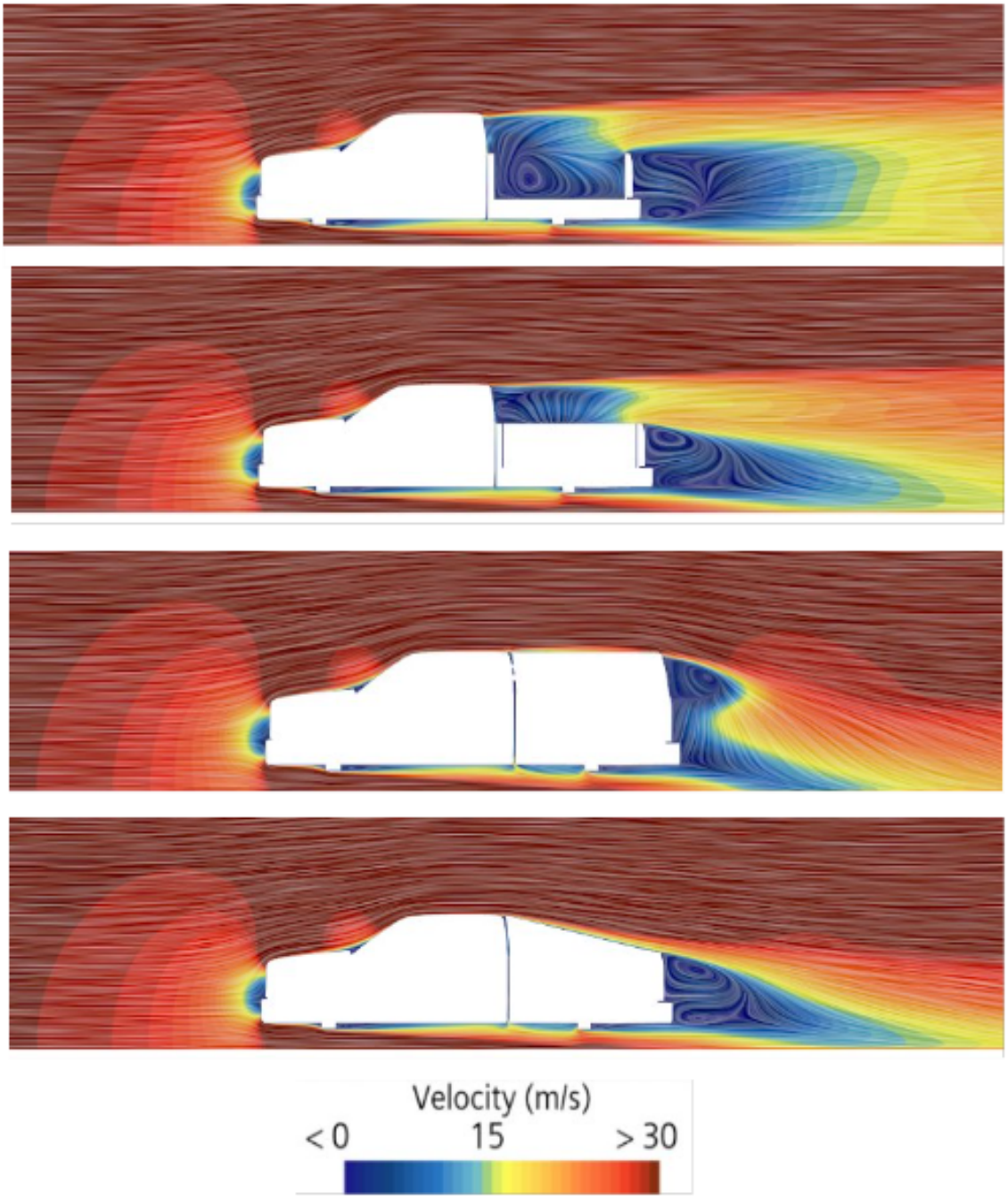

Figure 7.5: Velocity vector comparison between different configurations

The velocity vector graphs show the homogeneity of the velocity distribution on the surfaces with different back attachment configurations and the flow patterns around the vehicle. The baseline model's flow patterns are especially crucial since the wake pattern is disrupted and drag increases due to the trunk's openness and internal air circulation. By covering the trunk section with a solid block, the second configuration stops air from

moving inside the trunk. Consequently, by stabilizing the wake pattern and providing reduced drag counts compared to the previous model. By attaching the hatch back attachment to the rear, the third configuration reduces the drag force and extends the boundary layer connection. With smaller wake zones that benefit from lower drag force and more stable, improved flow patterns than previous setups, the fast back attachment is the final configuration.

7.4 Yaw angle testing

In computational fluid dynamics (CFD), yaw angle testing is an essential tool for forecasting an object's behavior in real-world scenarios where its axis of flow isn't always exactly aligned. It assists engineers in fine-tuning designs for enhanced performance, safety, and stability in a variety of scenarios, including maneuvering or crosswinds. The test simulations results have been plotted as below

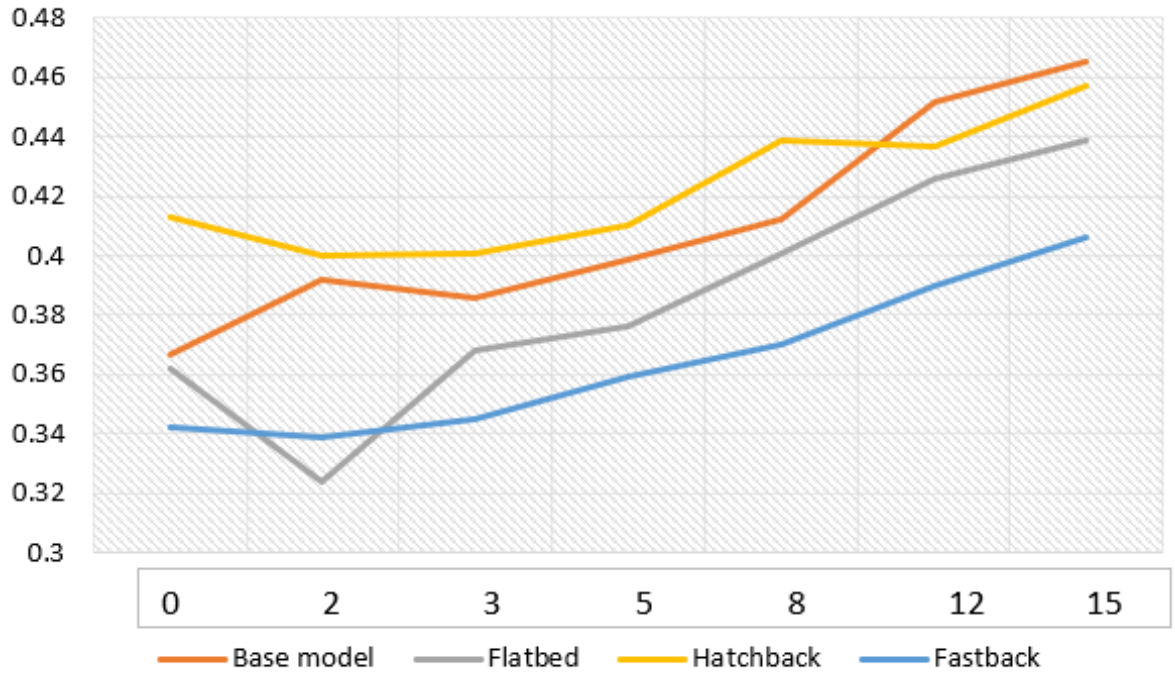

Figure 7.6: C_D comparison b/w the Configuration based CFD simulations

7.5 Wind Tunnel

The collected data from the wind tunnel testing was post-processed and analyzed as shown in 7.7. The results of the wind tunnel testing sessions are discussed in the next sections and compared with CFD simulations for better understanding. All the configurations were tested with 0°, 2°, 3°, 5°, 8°, 12°and 15°yaw angles in degrees, to investigate the behaviour of the vehicle at different side winds.

The manual rotation of the yaw bed in the wind tunnel adjustments introduces a margin

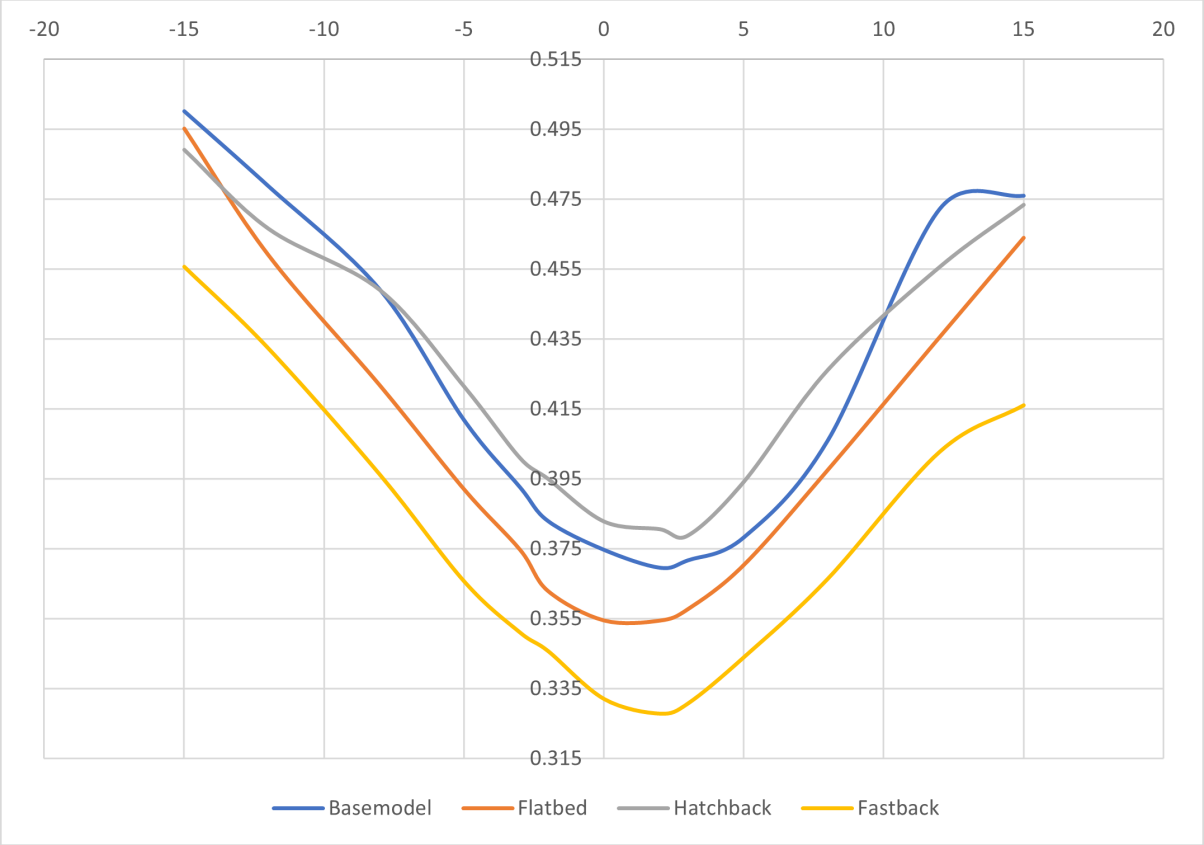

Figure 7.7: C_D comparison b/w the configuration based on wind tunnel data

of human error that can result in slight inaccuracies in setting the intended yaw angles, which is one of the reasons why the dip in the coefficient of drag C_D plot7.7 does not perfectly align with the 0°yaw angle. Even if they seem insignificant, these tiny variations can alter the aerodynamic data, making the dip seem at an angle that is somewhat different from actual zero. This disparity may be caused by alignment problems in the wind tunnel setup. Variations may be seen in the generated data if the vehicle or the yaw bed were not precisely centered or aligned with the wind tunnel's airflow axis.

Limitations in the measurement tools used to record aerodynamic data may also be a significant factor. Data may slightly move as a result of inaccurate readings or sensor drift during manual adjustments. Furthermore, results may be affected by small airflow asymmetries or intrinsic flow disturbances in the wind tunnel, which would move the point of lowest drag away from the actual zero. Last but not least, human method variations while manually adjusting each angle may introduce minute irregularities that impact the outcome. Together, these factors illustrate the difficulties in guaranteeing accuracy during manual wind tunnel testing and help explain why the dip in C_D does not line up exactly with the 0-degree yaw angle.

7.6 CFD vs Wind Tunnel Comparison

In this subsection the numerical results obtained from the Wind Tunnel tests and CFD simulations are compared and analysed.

7.6.1 Drag Coefficient

The coefficient of drag C_d of the Pick-up truck, as defined in equation (2.1), is calculated in both scenarios: wind tunnel tests and CFD simulations. Concerning wind tunnel tests, the C_d value requires correction according to equation (6.1), to account for blockage effects and the presence of walls. Since the the simulations and wind tunnel testing were from angle 0°to 15°, the blockage difference would not be major. So we have excluded the blockage factor while converting the Drag counts to C_d for each of the configuration(Base model, Flatbed, Hatchback and Fastback). Below are the results analyzed and plotted with comparison of the CFD simulation results v/s the wind tunnel testing results.

7.6.2 Base model:

Angle	**0**	**2**	**3**	**5**	**8**	**12**	**15**
BM	0.367	0.392	0.386	0.399	0.412	0.452	0.465
BM_WT	0.380	0.375	0.377	0.383	0.412	0.454	0.483

Table 7.1: Base model $C_D comparison$

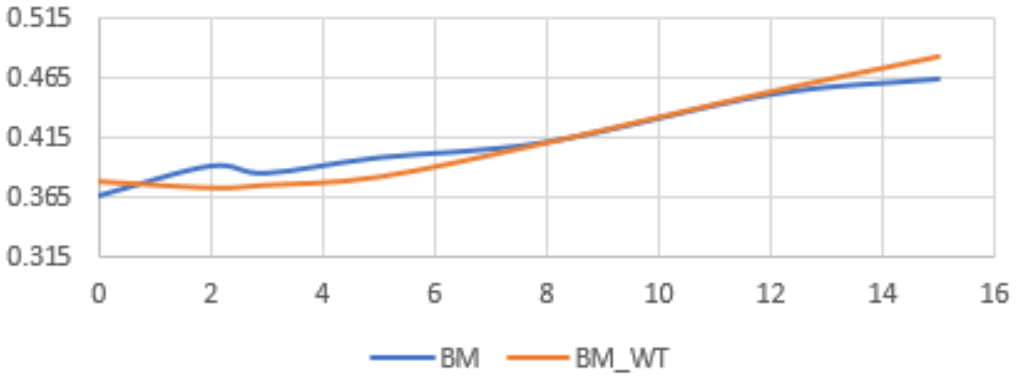

Figure 7.8: Base Model C_D Comparison of Yaw b/w CFD Simulation and WT Testing

The given data shows that the vehicle's coefficient of drag C_D increases as the yaw angle increases. The data for the two designs, Base model(BM) and Base model wind tunnel (BM-WT), show this pattern, which is consistent with aerodynamic principles. The coefficient of drag for (BM) is 0.367 and for (BM-WT) it is 0.380 at a yaw angle of 0°. Because of the vehicle's streamlined frontal area and generally smooth airflow, drag is reduced at this starting value, which is the baseline when the vehicle is facing the wind directly.

Both configurations exhibit a little increase in C_D when the yaw angle climbs to 2°and 3°, with BM displaying values of 0.392 and 0.386, respectively, and BM-WT showing a slight

dip before rebounding to 0.377 at 3°. This suggests that the air encounters resistance even at modest yaw angles because of the expanding effective frontal area and the first flow disturbances that emerge, which causes a slight rise in pressure drag.

The drag coefficient increases to 0.399 for BM and 0.383 for BM-WT when the yaw angle exceeds 5°, indicating that the airflow is now experiencing more noticeable disruptions. These disruptions, which are identified by the onset of flow separation on the vehicle's leeward side, increase the creation of turbulent wakes and pressure drag. At 8°, the effect is more pronounced, with both configurations aligning at 0.412, suggesting that as flow separation and turbulence increase, the effect of yaw on drag becomes more noticeable.

The coefficient of drag increases more noticeably at larger yaw angles, such 12°and 15°. While BM-WT exhibits a more pronounced increase to 0.454 and 0.483, respectively, the values for BM increase to 0.452 and 0.465. The increased turbulent vertices and enlarged low-pressure zones brought on by the leeward side's more extreme flow separation are the cause of these leaps. These effects are made worse by the air recirculation inside the car's trunk, which obstructs the fluid flow and increases drag even more. By trapping air in a cavity, the open trunk produces more eddies and recirculation zones, which amplify the separation effect and raise drag coefficients.

The combined impacts of increased exposure to the frontal area and disturbances to turbulent airflow are highlighted by this analysis of rising C_D with yaw angle. Resistance rises as the yaw angle increases because of the development of more pronounced flow separation and pressure differentials. This pattern in the given data shows how these dynamic and intricate flow features cause higher yaw angles to correlate with increasing aerodynamic inefficiency.

7.6.3 Flatbed model:

Angle	**0**	**2**	**3**	**5**	**8**	**12**	**15**
FB	0.362	0.324	0.368	0.376	0.401	0.426	0.439
FB_WT	0.359	0.359	0.363	0.375	0.403	0.442	0.470

Table 7.2: Flat bed model $C_D comparison$

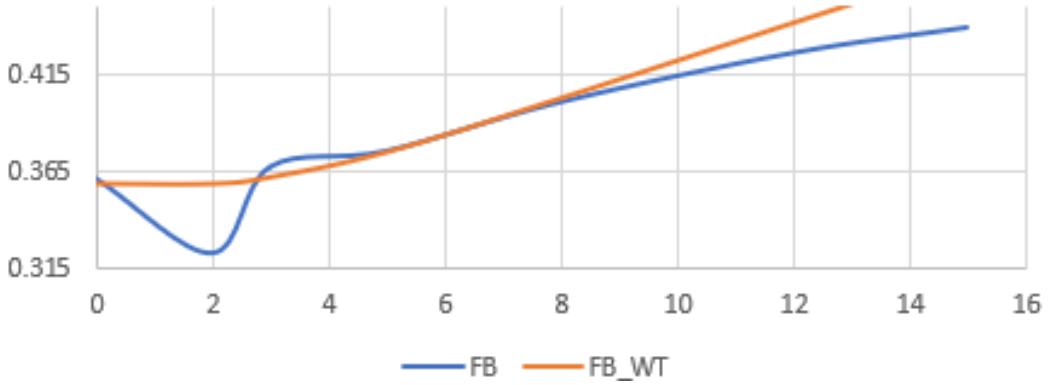

Figure 7.9: Flat Bed Model C_D Comparison of Yaw b/w CFD Simulation and WT Testing

Although it does so at generally lower values than the Base model (BM) and BM-WT configurations previously addressed, the coefficient of drag C_D in the Flatbed model(FB) and Flatbed wind tunnel model (FB-WT) designs likewise climbs as the yaw angle increases. The data shows this trend, with FB-WT starting at 0.359 and C_D for FB starting at 0.362 at a yaw angle of 0°. These starting values exhibit a modest decrease but are similar to those observed in the BM and BM-WT designs (0.367 and 0.380, respectively). This suggests that the trunk's flat-surface covering helps to improve overall aerodynamics by avoiding internal air recirculation.

For FB, an intriguing pattern is seen at a 2°yaw angle, where C_D falls to 0.324 before increasing once more to 0.368 at 3°. This abrupt dip is explained by the exceptionally smooth airflow surrounding the car at this angle, which momentarily lowers pressure drag until flow disturbances reappear. BM and BM-WT, on the other hand, do not exhibit this dip; rather, when the yaw angle increases from 0°to 3°, their C_D values continuously grow. This implies that the open trunk of the BM shape increases pressure drag and turbulence, particularly as the yaw angle starts to influence frontal area exposure and airflow disruption.

C_D for FB hits 0.376 and 0.401 when the yaw angle increases to 5°and 8°, respectively, whereas FB-WT records 0.375 and 0.403. The benefits of the flat-surface trunk cover in maintaining more stable flow and lowering drag-inducing turbulence are shown by these values, which show a continuous increase comparable to that observed in the BM configurations but stay lower overall. This relative decrease in C_D is partly due to the notable absence of air recirculation in FB and FB-WT, which was present in the BM configurations and resulted in increased flow separation and pressure drag.

The increase in C_D is more noticeable at higher yaw angles, such 12°and 15°, when FB records 0.426 and 0.439 and FB-WT reaches 0.442 and 0.470. These values are still lower than their BM and BM-WT equivalents (which peaked at 0.465 and 0.483), despite a noticeable increase that reflects the stronger impacts of flow disruptions and separation that are usual at bigger yaw angles. Because the sealed design in FB and FB-WT causes

less aerodynamic disturbance than the open trunk observed in BM, this highlights the significance of removing internal air recirculation within the trunk.

In conclusion, the FB and FB-WT designs have a more stable aerodynamic profile because of the flat trunk cover, even though both sets of configurations (FB/FB-WT and BM/BM-WT) exhibit an upward trend in C_D with increasing yaw angle because of increased frontal area exposure and flow separation. In comparison to the Base model configurations, this design feature lowers drag values overall by reducing turbulence caused by recirculation. The information and behavior show how little design adjustments can have a big impact on aerodynamic performance, especially at different yaw angles.

7.6.4 Hatchback model:

Angle	**0**	**2**	**3**	**5**	**8**	**12**	**15**
HB	0.413	0.4	0.401	0.410	0.439	0.437	0.457
HB_WT	0.388	0.386	0.384	0.399	0.432	0.462	0.480

Table 7.3: Hatch back model $C_D comparison$

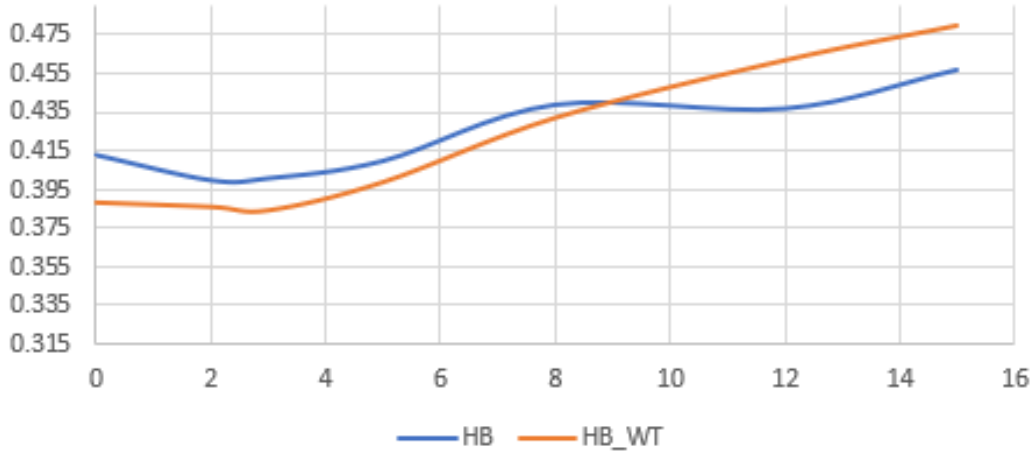

Figure 7.10: Hatch Back Model C_D Comparison of Yaw b/w CFD Simulation and WT Testing

Because of the aerodynamic difficulties brought about by the hatchback design, the flatbed (FB) and flatbed variants have lower coefficients of drag C_D than the hatchback (HB) and hatchback model wind tunnel (HB-WT) designs. The C_D for HB starts at 0.413 and the HB-WT at 0.388 at a yaw angle of 0°, which instantly indicates a higher baseline drag than the corresponding flatbed setups, which started at 0.362 (FB) and 0.359 (FB-WT). This first distinction highlights how the hatchback attachment complicates the aerodynamic profile of the car.

For HB, C_D marginally drops to 0.4 and 0.401 when the yaw angle rises to 2°and 3°, but for HB-WT, it hovers at 0.386 and 0.384. These values nevertheless exceed the corresponding FB values (0.324 at 2°and 0.368 at 3°for FB; 0.359 and 0.363 for FB-WT),

although being lower than at 0 degrees. This discrepancy demonstrates how the hatchback's design affects airflow, especially in the way it expands the frontal area, which more forcefully disturbs the air during yaw. Compared to the flatbed variants, the hatchback attachment creates a larger low-pressure area on the vehicle's leeward side, which is more difficult to control.

C_D for HB increases to 0.410 and 0.439 when the yaw angle increases to 5°and 8°, while HB-WT reaches 0.399 and 0.432. The usual trend of increased drag at higher yaw angles as a result of increased flow separation and intensified vortex formation is reflected in these increases. Reiterating the hatchback's function in producing a more noticeable wake behind the car, the HB configuration retains greater drag values than the FB and BM variants previously described. At corresponding yaw angles, the HB-WT layout likewise increases but retains lower values than the BM-WT, indicating that even while the hatchback increases drag, the BM's lack of recirculation still results in a modest decrease in C_D.

The drag values for HB increase to 0.437 and 0.457 at even larger yaw angles, such 12°and 15°, whereas HB-WT increases more noticeably to 0.462 and 0.480. These findings are in line with how BM and BM-WT behave at high yaw angles, where airflow disruptions and significant pressure drag take center stage. The hatchback stands apart, though, because to its special aerodynamic feature that expands the frontal surface exposed to the wind and expands the low-pressure area behind the car. The hatchback designs outperform the FB and FB-WT layouts, which at 15°achieved peak C_D values of 0.439 and 0.470, highlighting how the attachment raises overall aerodynamic resistance.

As a result of increased frontal area exposure and a larger low-pressure wake, the hatchback design in both HB and HB-WT configurations results in noticeably higher drag coefficients at all measured yaw angles when compared to the flatbed versions. Although less severe than in the open trunk configuration of the BM models, the hatchback nevertheless causes higher turbulent flow separation and pressure drag, which leads to increased aerodynamic inefficiency when compared to the more straightforward flatbed design. In terms of controlling airflow and lowering drag, this analysis emphasizes the significance of vehicle shape and rear design, with the hatchback clearly outperforming the flatbed in this area.

7.6.5 Fastback model:

Angle	**0**	**2**	**3**	**5**	**8**	**12**	**15**
FsB	0.342	0.339	0.345	0.359	0.37	0.39	0.406
FsB_WT	0.337	0.332	0.335	0.349	0.371	0.408	0.422

Table 7.4: Fast back model $C_D comparison$

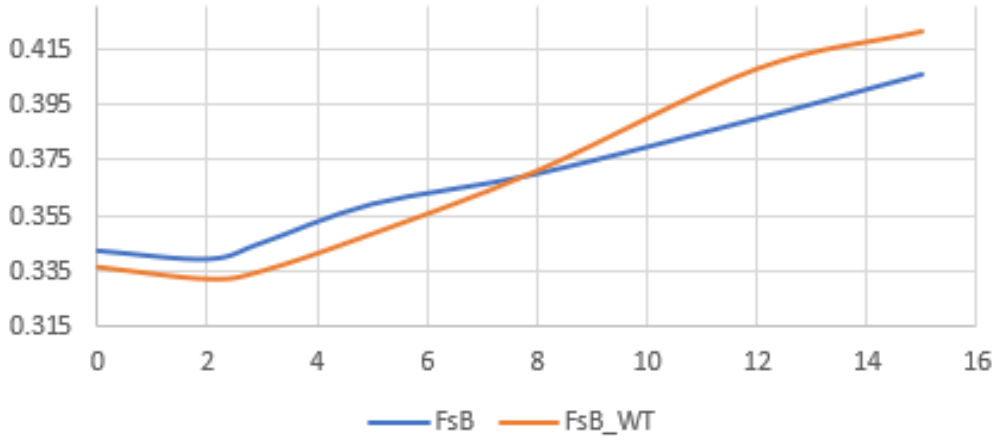

Figure 7.11: Fast Back Model C_D Comparison of Yaw b/w CFD Simulation and WT Testing

When compared to the other vehicle designs, the Fastback (FsB) and Fastback wind tunnel model (FsB-WT) configurations have the lowest coefficient of drag C_D at all tested yaw angles, indicating higher aerodynamic efficiency in both yaw and straight-line conditions. The C_D for FsB is 0.342 and the FsB-WT is 0.337, starting at a yaw angle of 0 degrees. These values are far lower than the baseline values seen in the Base model (BM), Hatchback (HB), and even the Flatbed (FB) configurations. This first benefit suggests that the streamlined profile of the fastback design effectively reduces drag when it is directly in line with airflow.

C_D for FsB just slightly changes when the yaw angle rises to 2°and 3°, first falling to 0.339 and then rising to 0.345. A similar pattern is shown in the FsB-WT, which records values of 0.332 and 0.335. The HB and BM setups, where there are more noticeable fluctuations because of the increased airflow disruption, stand in stark contrast to this smooth trend. As an illustration of the inefficiencies brought about by the greater low-pressure zone behind the hatchback attachment, HB's baseline C_D at 0 degrees was 0.413, which stayed comparatively high throughout the test range.

The FsB-WT registers 0.349 and 0.371 when the yaw angle hits 5°and 8°, while the FsB continues its slow increase to 0.359 and 0.370. These numbers are still behind those of BM, which also showed greater drag values, and HB, which reached 0.410 and 0.439. This suggests that the improved flow patterns of the fastback design minimize turbulent wake development and the pressure drag that goes along with it by maintaining more connected airflow along the body.

The benefits of the fastback design are even more noticeable at the greater yaw angles of 12°and 15°. While FsB-WT reaches 0.408 and 0.422, the C_D for FsB rises to 0.390 and 0.406. These numbers are still less than those seen in the BM and HB configurations, despite the fact that the increasing yaw angle inevitably results in an increase

in drag. For example, a greater low-pressure wake behind the vehicle and considerable flow separation caused the HB to reach 0.457 and 0.480 at these higher yaw angles. By encouraging smoother flow over its sloping rear profile, the fastback design reduces these disturbances, creating a smaller wake area and a less noticeable low-pressure zone.

Even at more extreme yaw angles, the FsB-WT configuration's tail addition serves to reduce drag by preserving coupled airflow and postponing flow separation. This characteristic demonstrates why the fastback design outperforms the hatchback and base variants, especially when it comes to the tail. The fastback shape directs airflow more efficiently and lessens the negative impacts of the hatchback's rear architecture, which produces significant turbulence and a wider area of low pressure.

In conclusion, when compared to the base model, hatchback, and flatbed layouts, the fastback design produces the best and lowest values under both straight and yaw scenarios. Better aerodynamic flow with a smaller low-pressure wake region is made possible by its design, which is particularly noticeable at greater yaw angles where drag tends to rise in previous arrangements. In all testing conditions, the fastback's sloped rear contributes to the maintenance of associated flow, which continuously reduces drag and improves aerodynamic performance.

Chapter 8

Conclusions

The main objective of this thesis research was to examine how a pickup truck's design, specifically its rear attachments, influences drag forces by analyzing the vehicle's aerodynamic performance. Computational Fluid Dynamics (CFD) simulations and wind tunnel testing were used to accomplish this. The tests' results were mostly in line with expectations, demonstrating that specific vehicle components particularly the front tracking points and special parts made a substantial contribution to the truck's overall drag force. Nevertheless, for the purposes of this investigation, the focus was mostly on the rear end alterations.

Four distinct rear attachment solutions were suggested by the study in an effort to increase the vehicle's aerodynamic efficiency. These designs' effects on the vehicle's performance were thoroughly examined by testing them in wind tunnels and using CFD models. Every new design was contrasted with the base model. The base was used as a point of comparison to evaluate how well the suggested adjustments worked. Understanding how the rear attachments affected the vehicle's overall aerodynamic behavior particularly with regard to drag reduction was the main goal.

When compared to the base model, three of the four studied designs showed appreciable drag reductions. The fastback arrangement was the most successful in reducing drag forces among them. Smoother detachment and reduced turbulence behind the vehicle were the results of this design's more efficient airflow, which was distinguished by a slanted rear attachment. When compared to the other designs, which also shown gains, to a lesser extent, the fastback's ability to minimize drag was note worthy.

The study examined the pickup truck's response to yaw and crosswind situations in addition to assessing its aerodynamic behavior in head-on wind conditions. Since cars seldom experience solely frontal wind in real-world scenarios, these variables were added to simulate more realistic driving circumstances. The findings demonstrated that the fastback layout maintained minimal drag forces and improved vehicle stability while continuing to function well in these diverse wind conditions. This demonstrated that the fastback design provided benefits in terms of aerodynamic efficiency under more difficult wind conditions in addition to assisting in lowering drag under normal circumstances.

Overall, this thesis research produced encouraging results. The outcomes of the CFD simulations and wind tunnel testing offered important new information about how comparatively minor adjustments to the vehicle's rear design could result in notable gains in aerodynamic performance. Additionally, the study advanced our knowledge of how various rear attachments affect a vehicle's overall aerodynamic performance, especially in yaw and crosswind situations. Future design optimizations that seek to strike a compromise between aerodynamic efficiency and vehicle functional requirements may benefit from this information, particularly when it comes to consumer and commercial vehicles like pickup trucks.

Chapter 9

Recommendations for future work

Yaw Angle Effect for more than 15° By continuing the study in order to comprehend how the vehicle may act in the event of strong cross winds, including yaw angle testing more than 15 degrees.

Design Modification with Longer body Length We looked at a middle range of body lengths for this thesis project; perhaps future research on longer body lengths may or may not produce better aerodynamic results. So the study on this would provide us with the better understanding on aerodynamics of pickup trucks.

Design Modification in Front part of the vehicle Since the front grill area of the vehicle has the highest stagnation point, as we discovered during our thesis project, improving the front portion of the vehicle may improve aerodynamics of the vehicle.

Chapter 10

References

1. Experimental Investigation of the Near Wake of a Pick-up Truck, Abdullah M. Al-Garni and Luis P. Bernal,University of Michigan Bahram Khalighi General Motors Corporation. [**https://www.researchgate.net/publication/242225829**]

2. CFD Simulations for Flow over Pickup Trucks, Zhigang Yang and Bahram Khalighi, General Motors Corporation [**https://www.researchgate.net/publication/296653478**]

3. Aerodynamics of a Pickup Truck: Combined CFD and Experimental Study Article in SAE International Journal of Commercial Vehicles · October 2009.
[**https://www.researchgate.net/publication/279157171**]